



## Original article

## Optical and electrical characteristics of p-type AlN co-doped ZnO thin films synthesized by RF sputtering

A. Ismail<sup>a</sup>, M.J. Abdullah<sup>b</sup>, M.A. Qaeed<sup>c</sup>, Mohammed A. Khamis<sup>d,\*</sup>, Bandar Ali AL-Asbahi<sup>e,f</sup>, Saif M. Qaid<sup>e,g</sup>, W.A. Farooq<sup>e</sup><sup>a</sup> Department of Physics, University of Hafr Al Batin, 31991, Saudi Arabia<sup>b</sup> School of Physics, Universiti Sains Malaysia, 11800 Penang, Malaysia<sup>c</sup> Department of Physics, Faculty of Science, University of Jeddah, Saudi Arabia<sup>d</sup> Department of Petroleum and Natural Gas Engineering, King Saud University, Saudi Arabia<sup>e</sup> Department of Physics & Astronomy, College of Sciences, King Saud University, Saudi Arabia<sup>f</sup> Department of Physics, Faculty of Science, Sana'a University, Yemen<sup>g</sup> Department of Physics, Faculty of Science, Ibb University, Yemen

## ARTICLE INFO

## Article history:

Received 22 October 2019

Revised 25 October 2020

Accepted 28 October 2020

Available online 05 November 2020

## Keywords:

Optical properties

Zinc oxide

X-ray diffraction

Electrical properties

## ABSTRACT

Zinc oxide (ZnO) has attracted significant interest due to its exceptional material characteristics like its wide band gap (3.37 eV) and the high exciton binding energy. However, the application of ZnO is constrained by the difficulty in obtaining P-type samples. In this study, p-type ZnO thin films were fabricated using the co-doping technique with ZnO and AlN targets. Different RF powers were used for ZnO to deposit the films. However, the power on AlN target was fixed at 90 W. The structural, optical and electrical properties of the prepared films were inspected. The results of XRD showed that all the films exhibited ZnO (002) peak of wurzite structure. The UV emission peaks (3.24 eV–3.53 eV) identified in PL spectra is possibly due to the recombination of free excitons. The Raman peaks which shown at 576.22 cm<sup>-1</sup> and 274 cm<sup>-1</sup> denote ZnO:AlN and ZnO:N respectively. The Hall measurements of the films deposited at RF powers of 250 W and 200 W for ZnO target exhibited n-type conduction with corresponding mobilities of 2.75 cm<sup>2</sup> V<sup>-1</sup> s<sup>-1</sup> and 1.58 cm<sup>2</sup> V<sup>-1</sup> s<sup>-1</sup> respectively with electron concentrations of 2.35 × 10<sup>18</sup> cm<sup>-3</sup> and 5.26 × 10<sup>18</sup> cm<sup>-3</sup>, respectively. However, the films deposited using RF powers of (150, 175) W and 225 W for ZnO target exhibited p-type conduction with hole concentrations of 2.14 × 10<sup>17</sup> cm<sup>-3</sup>, 2.37 × 10<sup>19</sup> cm<sup>-3</sup> and 3.68 × 10<sup>21</sup> cm<sup>-3</sup> with corresponding mobilities of 9.21 cm<sup>2</sup> V<sup>-1</sup> s<sup>-1</sup>, 0.129 cm<sup>2</sup> V<sup>-1</sup> s<sup>-1</sup> and 3.41 × 10<sup>-3</sup> cm<sup>2</sup> V<sup>-1</sup> s<sup>-1</sup> respectively. Therefore, RF power values of (150, 175) W and 225 W might be ideal for dopants activation to obtain p-type ZnO.

© 2020 The Authors. Published by Elsevier B.V. on behalf of King Saud University. This is an open access article under the CC BY-NC-ND license (<http://creativecommons.org/licenses/by-nc-nd/4.0/>).

## 1. Introduction

In recent times, Zinc oxide (ZnO) has garnered significant attention due to its exceptional material properties that include wide band gap (3.37 eV) and high exciton binding energy (60 meV), which makes it suitable for a wide array of applications like gas sensors and solar cell applications (Ozgur et al., 2005, Lau, 2005,

Alivov et al., 2003). However, the complexity of obtaining P-type ZnO samples effect in the application of ZnO in optoelectronics. ZnO is characterized by n-type conductivity as a result of oxygen vacancies and zinc interstitial. For ZnO p-type, Nitrogen has been treated as an option for doping ZnO. However, ZnO has a low N solubility, which introduces a relatively deep acceptor level. To reduce the acceptor ionization energy and to improve the solubility of N in ZnO, Yamamoto (Yamamoto, 2002) proposed a codoping technique to get p-ZnO.

ZnO thin films could be synthesized using a different techniques like (RF) sputtering (Rusu et al., 2007, Hezam, 2007, Ohgaki et al., 2003, Ryu and Zhu, 2000). The technique of RF sputtering has attracted immense interest as the properties of the ZnO films can be regulated by modifying the sputtering conditions. This is imperative since the structural, electrical and ZnO films optical

\* Corresponding author.

E-mail address: [mokhamis@ksu.edu.sa](mailto:mokhamis@ksu.edu.sa) (M.A. Khamis).

Peer review under responsibility of King Saud University.



properties are dependent on the conditions of preparation like substrate type, film thickness, deposition pressure, substrate temperature, RF power and annealing temperature, as reported in earlier studies (Ismail and Abdullah, 2013a, Ismail and Abdullah, 2013b, Ismail and Abdullah, 2013c, Ismail et al., 2015). Therefore, this study fabricates p- type ZnO thin films using the co-doping technique with ZnO and AlN targets. To determine the effect of modifying preparation conditions, the films were deposited at different RF powers for ZnO target. However, the power on AlN target was fixed at 90 W.

## 2. Experimental

AlN co-doped ZnO thin films were synthesized on type n-Si (100) and glass slide substrates through RF sputtering, by means of high purity ZnO target and high purity of AlN target. Acetone was used to wash the substrates and isopropanol in an ultrasonic bath for a duration of 15 min then subsequently rinsed with deionized water. Afterwards, Edwards A500 RF sputtering unit was used where the substrates were fixed to a rotating substrate holder, which is placed at 10 cm distance above the ZnO target. Argon (Ar) and Nitrogen (N<sub>2</sub>) of high purity (99.99%) were utilized for the sputtering of the target. Nitrogen and Argon were combined at a ratio of 80:20 to prepare the thin films. The pressure inside the chamber was maintained at  $2 \times 10^{-2}$  mbar throughout the sputtering process. Then, the films were deposited at 90 W for the AlN target and at different RF powers for ZnO target for about 50 min. The conditions of the AlN co-doped ZnO films deposition were shown in Table 1.

The films optical properties were examined using Raman spectroscopy, UV-visible spectrophotometry, and Photoluminescence (PL) and. The prepared films thickness (t) was determine using F20 filmetrics. The structural thin films properties were characterized using X-ray diffractometer (source Cu K<sub>α</sub> with  $\lambda = 1.5406 \text{ \AA}$ ), while the fabricated ZnO thin films surface morphologies were studied using field emission scanning electron microscopy (FESEM). The samples electrical properties were investigated using the Hall Effect equipment (HL5500PC model).

## 3. Results and discussion

The prepared thin films thickness (t) was observed to be increase with the applied RF powers on ZnO target as shown in Fig. 1. This indicates that the amount of sputtered atoms from the target is proportional to the applied RF power.

The XRD spectra for the synthesized AlN doped ZnO films is shown in Fig. 2. The current research is comparing the XRD spectra for AlN doped ZnO with the undoped ZnO in a previous work (Ismail and Abdullah, 2013a, Ismail and Abdullah, 2013b, Ismail and Abdullah, 2013c). It was found that the (002) ZnO phase is discernible in all the films and the average value of  $2\theta$  and d of the

**Table 1**

Prepared conditions of AlN: ZnO thin films at different powers on Si and glass substrates.

| Deposition parameters  | Conditions   |
|------------------------|--|
| Operation pressure     | 0.02 mbar  |
| Sputtering gases       | (Ar: (N <sub>2</sub> ) = (20:80)   |
| Power on targets       | ZnO target ≡ (250, 225, 200, 175 and 150)W with AlN target ≡ 90 W<br>Samples (ANZO41, ANZO40, ANZO39, ANZO38 and ANZO37) correspondingly |
| Deposition temperature | Room temperature   |

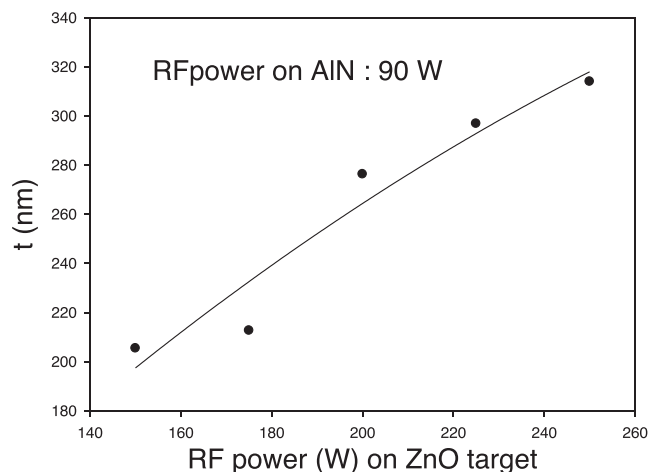


**Fig. 1.** Thickness of AlN: ZnO thin films as a function of RF power on Si substrates.

undoped ZnO is equal to  $34.1841^\circ$  and  $2.6229 \text{ \AA}$  respectively (Ismail and Abdullah, 2013a, Ismail and Abdullah, 2013b, Ismail and Abdullah, 2013c). The AZO 40 sample displayed the lowest d-spacing value of  $0.26174 \text{ nm}$  comparing with the undoped ZnO, which can be attributed to the Al ions substitution with Zn ions where the radius of Al<sup>3+</sup> ion ( $0.53 \text{ \AA}$ ) is smaller than the radius of Zn<sup>+2</sup> ion ( $0.74 \text{ \AA}$ ). Therefore, the (002) peak position of the AZO 40 sample shifted to a higher diffraction angle. Secondly, the sample showed the smallest calculated value of the FWHM of ZnO (002) peak comparing with the other samples. So, the abnormal behavior in the crystallite size was shown for AZO40 sample. However, the d-spacing value of AZO 37, AZO 38, AZO 39 and AZO 41 samples is larger than the d-spacing value of the undoped ZnO, probably due to the substitution of N<sup>-3</sup> ions on O<sup>-2</sup> ions site, where the radius of N<sup>-3</sup> ion ( $1.46 \text{ \AA}$ ) is larger than the radius of O<sup>-2</sup> ion ( $1.40 \text{ \AA}$ ). Therefore, the (002) peak position shift to a smaller angle. FWHM of ZnO (002) peak was used to calculate the crystallite size (D) in the synthesized thin films using the following Scherrer's formula.

$$D = 0.94 \lambda / (\beta \cos\theta)$$

where  $\theta$  is the Bragg angle,  $\lambda$  denotes the incident X-ray wavelength and  $\beta$  represents the full width at half maximum (FWHM). Table 2 summarizes the values found from XRD technique for (002) AlN: ZnO thin films phase.

The AlN: ZnO films EDX analysis are presented in Table 3, where minor concentrations of nitrogen (0.09–3.96 at %) was identified. It also important to notice that N and Al were incorporated at different concentration into the prepared AlN: ZnO thin films although the RF sputtering power on AlN was fixed at 90 W. This could be explained as following, introduction of nitrogen during the fabrication process (80%N<sub>2</sub>:20%Ar) and using different powers in ZnO target could have eventually led to the formation of (N<sub>2</sub>)<sub>O</sub> donors or (N)<sub>O</sub> acceptors in the films resulting in different concentration of N in the prepared thin films. The other possible mechanism is due to the formation of N-Al-N complex, arising from Al<sub>Zn</sub> (Al on Zn) and N<sub>O</sub> (N on O) according to the suggestions of Yamamoto's model. This configuration (N-Al-N) can stabilize ionic charges, enhances strong attractions between donor (Al) and acceptor (N) and reduces the repulsive interactions between the acceptors. In addition, the binding energy of the donor can be raised and the binding energy of the acceptor can be reduced, resulting in shallower acceptor that could improve the solubility of N-Al-N complex in the prepared of ZnO films (Yamamoto, 2002). The films surface morphology was measured using FESEM (Fig. 3). As

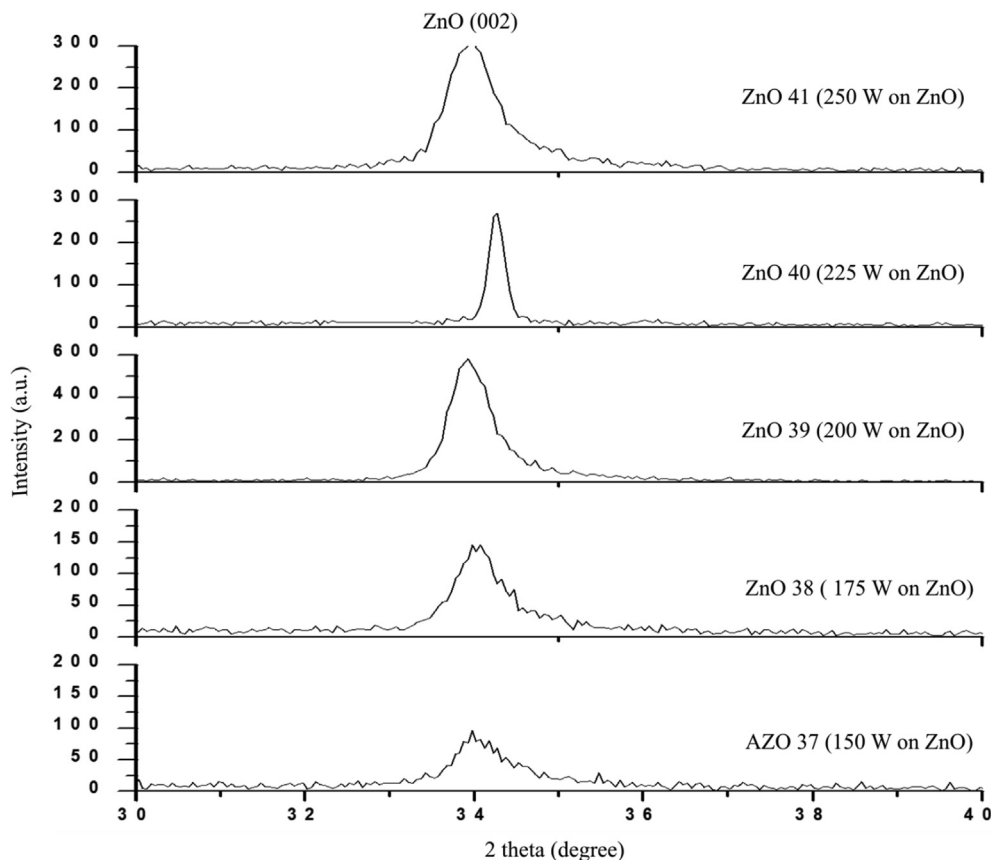


Fig. 2. XRD spectra of AlN: ZnO thin films at a different of RF power on Si substrates.

Table 2

Data summary from XRD of AlN: ZnO thin films at a different RF power on Si substrates.

| Sample | 2 θ (°) | FWHM(°) | d (Å)  | c (Å)  | D(nm) |
|--------|---------|---------|--------|--------|-------|
| AZO 37 | 33.9659 | 0.3936  | 2.6394 | 5.2788 | 22.05 |
| AZO 38 | 34.0759 | 0.3936  | 2.6311 | 5.2622 | 22.06 |
| AZO 39 | 33.8877 | 0.3936  | 2.6453 | 5.2906 | 22.05 |
| AZO 40 | 34.2604 | 0.1968  | 2.6174 | 5.2348 | 44.14 |
| AZO 41 | 34.0228 | 0.3936  | 2.6351 | 5.2702 | 22.06 |

Table 3

EDX analysis of AlN: ZnO films at different RF powers on Si substrates.

| Sample | NK (at %) | O K (at %) | Al K (at %) | Zn L (at %) |
|--------|-----------|------------|-------------|-------------|
| AZO 37 | 3.59      | 55.17      | 3.66        | 37.59       |
| AZO 38 | 0.09      | 56.27      | 4.92        | 38.73       |
| AZO 39 | 3.10      | 54.43      | 2.81        | 39.66       |
| AZO 40 | 3.96      | 53.72      | 2.91        | 39.41       |
| AZO 41 | 2.76      | 51.18      | 2.07        | 43.99       |

observed in the FESEM images, the particles of the thin films grew larger as the RF power applied on ZnO target increased.

Ultraviolet and visible (UV–vis) transmission spectrometer (model: U-2000 HITACHI) was used to determine the energy band gap ( $E_g$ ). The light produced by light grating is splitted in to two equal intensity beams (reference beam and sample beam) using a half mirror. Then, the two beams passed through the reference and the sample cuvettes and their intensities are then measured by the detectors. The intensity of the reference beam is defined

as  $I_0$  and the intensity of the sample beam is defined as  $I$ . The ratio ( $I/I_0$ ) is defined as the transmittance ( $T_i$ ). The relation between the absorption coefficients  $\alpha$  determined from the transmittance spectra and the photon energy ( $E$ ) is given by;

$$\alpha E = A(E - E_g)^{1/2}, \quad \alpha = \frac{1}{t} \ln\left(\frac{1}{T_i}\right)$$

where  $E_g$  is the energy band gap of the semiconductor,  $t$  is the thickness of the films and  $A$  is a constant. Therefore, a plot of  $(\alpha E)^2$  versus photon energy  $E$  produced a straight line that cut the photon energy axis at the energy band gap value. The photon energy can be calculated using the following equation:

$$E \text{ (eV)} = \frac{hc}{\lambda} = \frac{1240}{\lambda \text{ (nm)}}$$

where  $h$  is the planck’s constant,  $c$  is the speed of light in vacuum and ( $\lambda$ ) is the wavelength.

Fig. 4 revealed a good optical transmittance of ZnO doped with AlN thin films that exceeds 70% in the visible range. Also, it is important to notice from the XRD analysis that, only AZO 40 sample displayed d-spacing value of 0.26174 nm which was smaller than the d-spacing of the undoped ZnO (0.26229 nm) (Ismail and Abdullah, 2013a, Ismail and Abdullah, 2013b, Ismail and Abdullah, 2013c). Secondly, AZO 40 showed the largest value of the crystallite size of (44.14 nm) comparing with the other samples (AZO37, AZO38, AZO39 and AZO41). So, a different behavior in UV–vis spectra for this samples was shown which could be attributed to the substitution of Zn ions with Al ions.

Fig. 5 displays the graph of  $(\alpha E)^2$  versus  $E$  for the prepared samples that produces a direct energy band gap values of 3.31 eV, 3.40 eV, 3.39 eV, 3.41 eV and 3.40 eV for the prepared films with

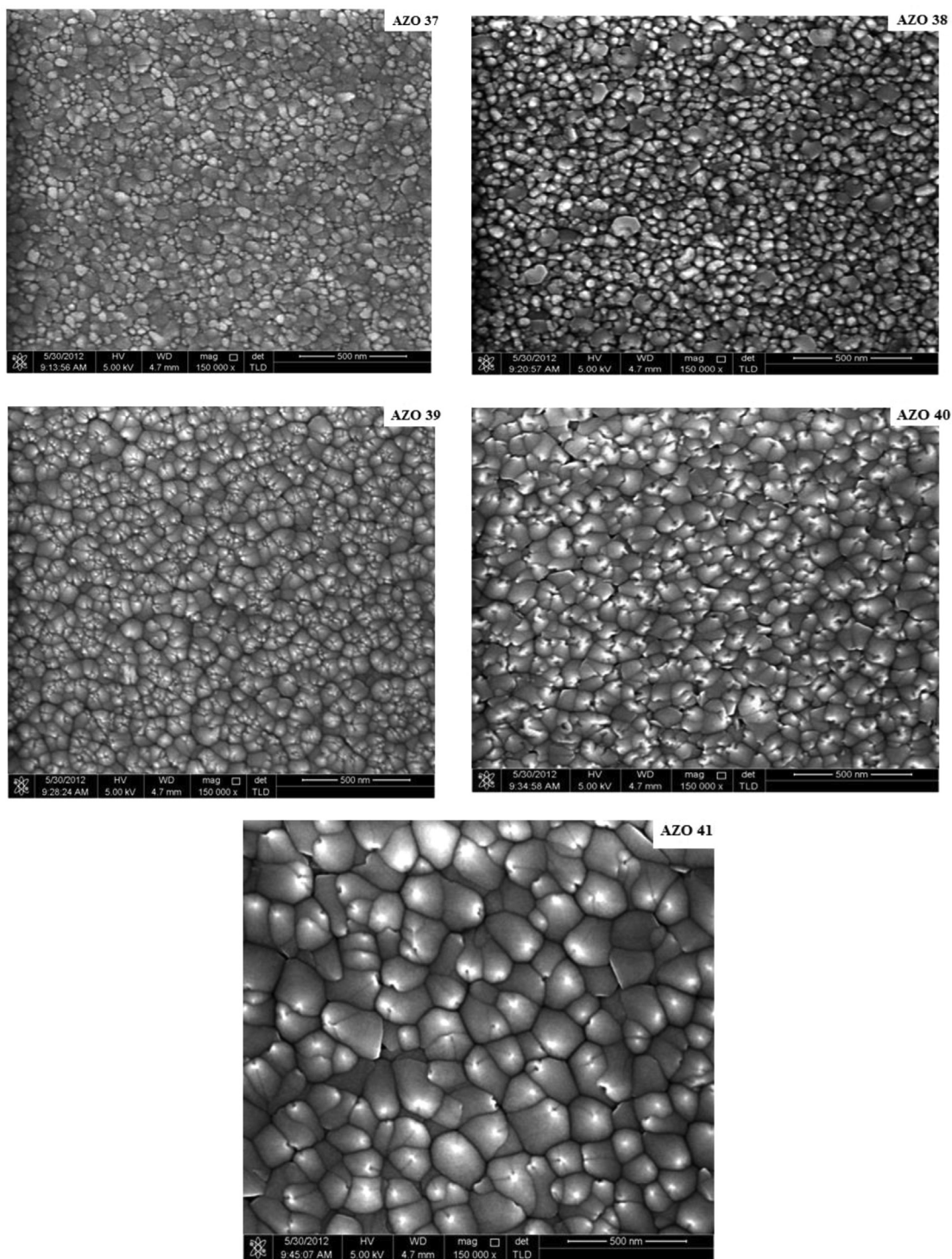


Fig. 3. FE-SEM images of AlN: ZnO thin films at different RF powers on Si substrates.

RF power (ZnO target) of 250, 225, 200, 175 and 150 W, respectively. As shown in Fig. 6, the optical direct energy band gap shifted from 3.41 eV to 3.31 eV with decreasing Al concentration, which is consistent with earlier related reports (Zi-qiang et al., 2006, Burstein, 1954, Moss, 1954), and is referred to as the Burstein-Moss effect.

The photoluminescence (PL) characteristics of the prepared AlN:ZnO thin films were obtained at room temperature in the photon energy range of 1.24 eV–4.1 eV. All the films showed UV emission peaks (Fig. 7) attributed to the free exciton recombination

indicating a good crystalline structure and also good optical properties (Ismail and Abdullah, 2013a, Ismail and Abdullah, 2013b, Ismail and Abdullah, 2013c, Kumar et al., 2009). Due to the Moss-Burstein effect the UV emission bands shifted to higher energy (from 3.26 eV to 3.53 eV) with increase in Al concentration from 2.07% to 3.66% which is in conformity with the optical transmittance results. It is important to see that the green emission (2.1 eV–2.3 eV) in the present films show low intensity of (100–180 a.u.) in comparing with our published undoped ZnO (450–1000 a.u.) (Ismail and Abdullah, 2013a, Ismail and Abdullah, 2013b, Ismail

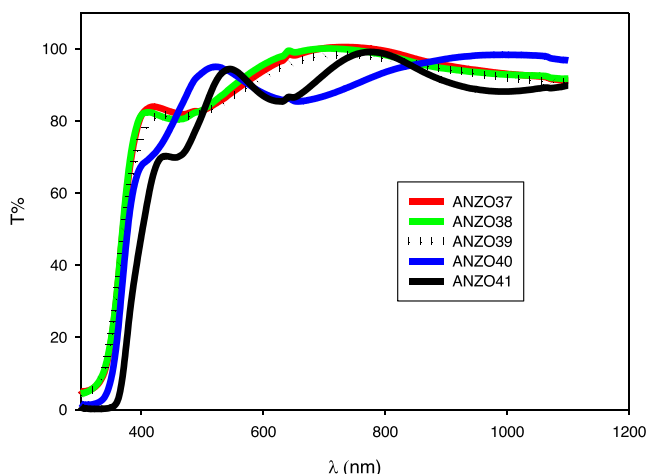


Fig. 4. AIN: ZnO Transmittance spectra of the prepared thin films on glass substrates at different RF powers.

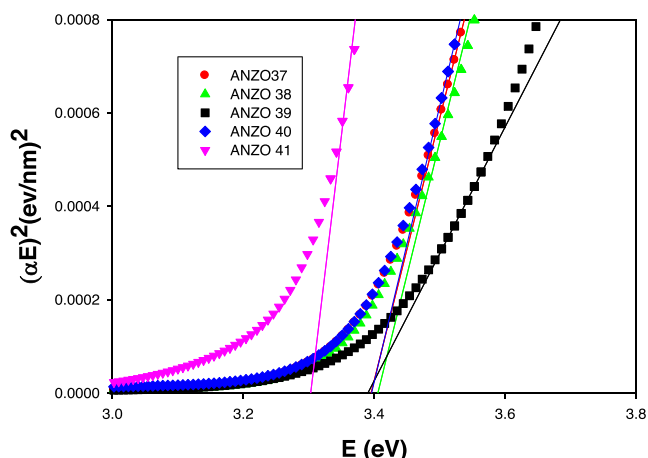


Fig. 5.  $(\alpha E)^2$  versus E of AIN: ZnO films on glass at various RF powers on glass substrates.

and Abdullah, 2013c). The lowering of the intensity indicate the successes doping of AIN: ZnO and also reducing the effect of the intrinsic defects in this films (Kumar et al., 2014, Verma et al., 2015). As a result, the dopant-induced in ZnO films will be effect in the electrical properties as will be shown latter.

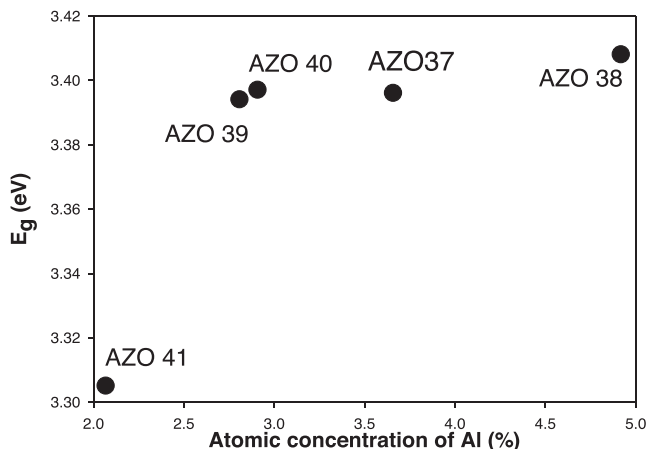


Fig. 6. Direct energy gap ( $E_g$ ) versus Al at % concentration of AIN: ZnO thin films at different RF powers on glass substrates.

The AIN doped ZnO thin films Raman spectra is shown in Fig. 8 (a). It is important to detect in the present work a new peak at  $274\text{ cm}^{-1}$  for all the prepared thin film samples which was not shown in the undoped ZnO. This peak denoted to the presence of nitrogen in all the prepared samples (Zhao et al., 2010). Whereas there is a shift in the peak which was observed at  $576.22\text{ cm}^{-1}$  in the present research comparing with the previous work for undoped ZnO ( $573.72\text{ cm}^{-1}$ ) (Ismail and Abdullah, 2013a, Ismail and Abdullah, 2013b, Ismail and Abdullah, 2013c). This shift indicate the successes doping of AIN :ZnO films which is attributable to A1 (LO) modes in agreement with other published work (Zhao et al., 2010, Cerqueira et al., 2010). These modes intensity ( $274\text{ cm}^{-1}$  and  $576.22\text{ cm}^{-1}$ ) are linearly related to the concentration of the nitrogen, which is a valuable tool for evaluating the relative nitrogen concentration in the films (Kaschner et al., 2002). Thus, it can be inferred that incorporation of nitrogen into the ZnO films is influenced by the magnitude of RF power applied on ZnO target. However, it is imperative to note that there is a disparity between the results of Kascher (Kaschner et al., 2002) and the EDX (Table 3) presented in this study, since the EDX presented results only at one point on the samples and offered primary information on the nitrogen in the samples. Nonetheless, this research seems to be more consistent with that of Kascher (Kaschner et al., 2002) who introduced more accurate results which could be used to find the relative concentration of nitrogen in the films.

The electrical properties of the synthesized AIN doped ZnO thin films (n-type and p-type conductivities) are presented in Table 4. The concentration, resistivity and mobility of the carrier were measured as a function of RF powers on ZnO target. AZO 37, AZO 38 and AZO 40 samples displayed p-type conductivity with hole concentrations of  $2.14 \times 10^{+17}\text{ cm}^{-3}$ ,  $2.37 \times 10^{+19}\text{ cm}^{-3}$  and  $3.68 \times 10^{+21}\text{ cm}^{-3}$  respectively. The p-type conductivity in the AZO 40 sample can be attributed to the substitution of  $\text{Zn}^{+2}$  ions site ( $0.074\text{ nm}$ ) with  $\text{Al}^{+3}$  ions ( $0.053\text{ nm}$ ) and the development N-Al-N complex which serves as a shallow acceptor. This is corroborated by the presence or incidence of nitrogen in the sample as deduced from the XRD, Raman and EDX results as well as the lesser d-spacing value ( $0.26174\text{ nm}$ ) compared to that of undoped ZnO ( $0.26229\text{ nm}$ ). On the other hand, the p-type conductivity in AZO 37 and AZO 38 samples can be attributed to the substitution of  $\text{O}^{-2}$  ions site ( $0.140\text{ nm}$ ) with  $\text{N}^{-3}$  ions ( $0.146\text{ nm}$ ) and the development of  $(\text{N}_2)_\text{O}$  donors and  $(\text{N})_\text{O}$  acceptors. Nevertheless,  $(\text{N})_\text{O}$  acceptors effect more than of  $(\text{N}_2)_\text{O}$  donors effect , leading to the creation of p-type conductivity in these samples. This is confirmed by the presence of nitrogen detected by Raman, XRD, EDX results, and the larger d-spacing values of the samples ( $0.26394\text{ nm}$  and

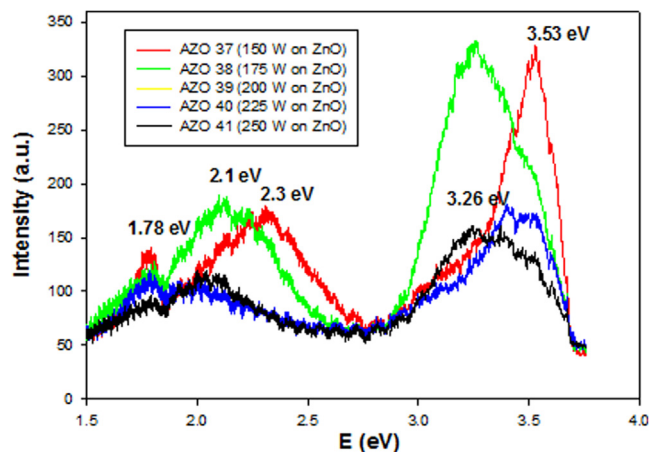


Fig. 7. The PL spectra of AIN: ZnO thin films at different RF powers on Si substrates.

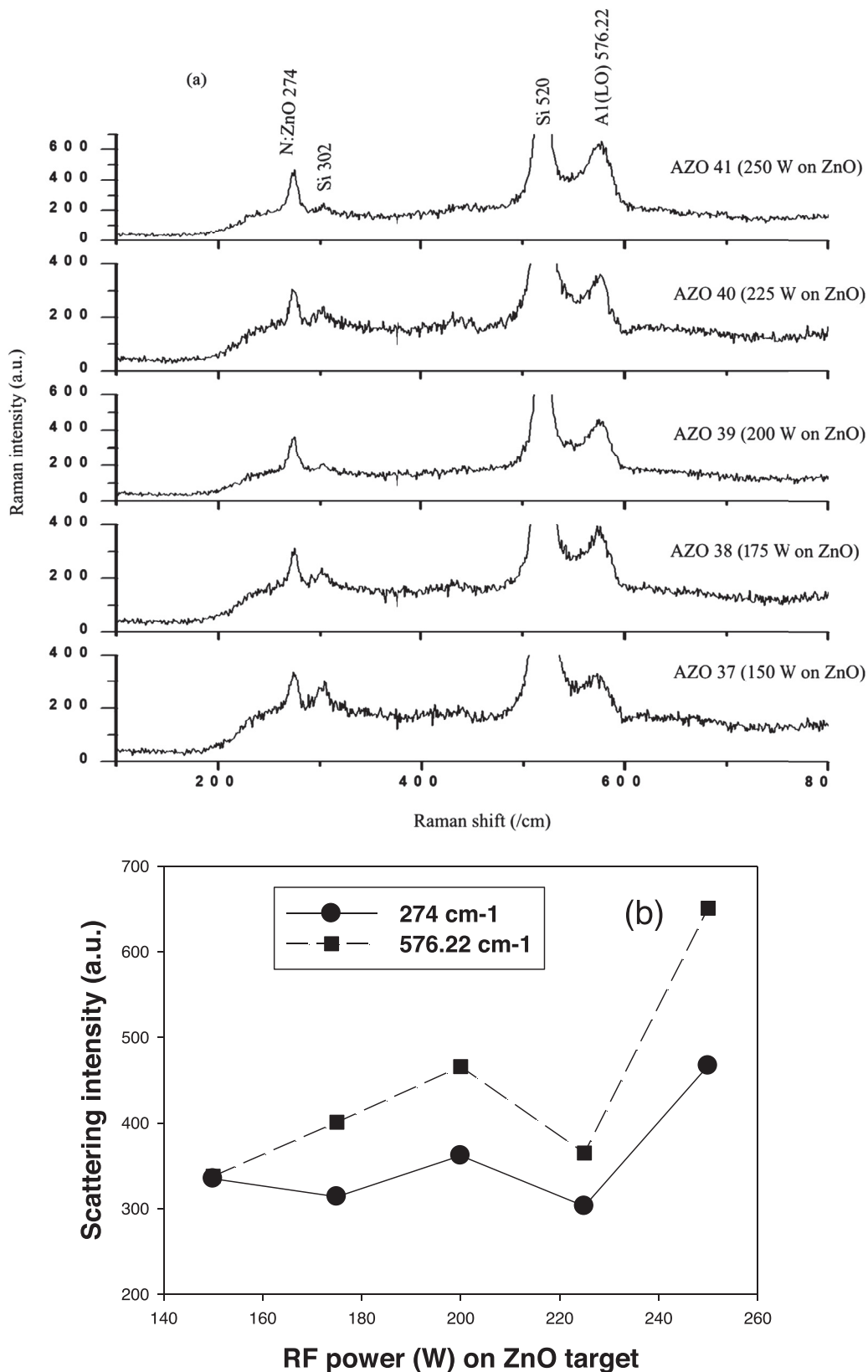


Fig. 8. (a) Raman spectra of AlN: ZnO thin films and (b) modes intensity variation at different RF on Si substrates.

0.26311 nm, respectively) as compared to that of the pristine/undoped ZnO (0.26229 nm).

Conversely, the AZO 39 and AZO 41 samples displayed n-type conductivity with electron concentrations of  $5.26 \times 10^{18} \text{ cm}^{-3}$  and  $2.35 \times 10^{18} \text{ cm}^{-3}$ , respectively. Raman, XRD and EDX results

confirmed the presence of nitrogen in these samples. In addition, the larger d-spacing values of the samples (0.26453 nm and 0.26351 nm, respectively) as compared to that of undoped ZnO (0.26229 nm) implies  $\text{N}^{3-}$  ions substituted  $\text{O}^{2-}$  ions. Nonetheless, the effect of  $(\text{N}_2)_\text{O}$  donors and the other intrinsic donors exceeds

**Table 4**  
Electrical properties of AlN: ZnO thin films prepared at different RF powers on Si substrates.

| Sample | Thickness, t (nm) | Resistivity ( $\Omega\text{cm}$ ) | Mobility ( $\text{cm}^2 \text{V}^{-1} \text{s}^{-1}$ ) | Carrier concentration ( $\text{cm}^{-3}$ ) |
|--------|-------------------|-----------------------------------|--|--|
| AZO37  | 210               | 3.170                             | 9.21   | $+2.14 \times 10^{+17}$                    |
| AZO38  | 220               | 2.040                             | 0.129  | $+2.37 \times 10^{+19}$                    |
| AZO39  | 276               | 0.751                             | 1.58   | $-5.26 \times 10^{+18}$                    |
| AZO40  | 280               | 0.498                             | $3.41 \times 10^{-3}$                                  | $+3.68 \times 10^{+21}$                    |
| AZO41  | 314               | 0.966                             | 2.75   | $-2.35 \times 10^{+18}$                    |

that of  $(\text{N})_{\text{O}}$  acceptors, leading to the formation of n-type conductivity in these samples. From Raman spectra, the dependence of mode intensity on the RF power applied to ZnO is presented in Fig. 8 (b). It can be deduced that nitrogen absorption into the samples increases with higher RF power of ZnO, possibly due to higher intensity of  $274 \text{ cm}^{-1}$  and  $576.22 \text{ cm}^{-1}$  modes for ZnO:N and ZnO:AlN, respectively. Therefore, RF power values of (150, 175 and 225) W may be ideal conditions to obtain p-type ZnO.

#### 4. Conclusion

The p-type ZnO was obtained via the co-doping of AlN and ZnO. The deposition of the films for ZnO target was occurred at different RF powers of (150, 175, 200, 225 and 250) W and 100 W for AlN target. All the films exhibited ZnO (002) peak of wurzite structure. The observed Raman peaks of  $274 \text{ cm}^{-1}$  and  $576.22 \text{ cm}^{-1}$  are associated with the incorporation of N and AlN in the ZnO films. From Hall measurements, the deposited thin films at RF powers of (150, 175 and 225) W for ZnO target and 90 W for AlN target exhibit conduction of p-type with hole concentrations of  $2.14 \times 10^{+17} \text{ cm}^{-3}$ ,  $2.37 \times 10^{+19}$  and  $3.68 \times 10^{+21} \text{ cm}^{-3}$  with corresponding mobilities of  $9.21 \text{ cm}^2 \text{V}^{-1} \text{s}^{-1}$ ,  $0.129 \text{ cm}^2 \text{V}^{-1} \text{s}^{-1}$  and  $3.41 \times 10^{-3} \text{ cm}^2 \text{V}^{-1} \text{s}^{-1}$ , respectively. The p-type conductivity in the AZO40 (225 W) sample can be attributed to the substitution of  $\text{Zn}^{+2}$  ions site (0.074 nm) with  $\text{Al}^{+3}$  ions (0.053 nm) as confirmed using XRD and the development N-Al-N complex which serves as a shallow acceptor. For AZO37(150 W) and AZO38 (175 W) samples, the p-type conductivity can be attributed to the substitution of  $\text{O}^{-2}$  ions site (0.140 nm) with  $\text{N}^{-3}$  ions (0.146 nm) and the development of  $(\text{N}_2)_{\text{O}}$  donors and  $(\text{N})_{\text{O}}$  acceptors. Nevertheless,  $(\text{N})_{\text{O}}$  acceptors effect more than of  $(\text{N}_2)_{\text{O}}$  donors effect, leading to the creation of p-type conductivity in this samples.

#### Declaration of Competing Interest

The authors declare that they have no known competing financial interests or personal relationships that could have appeared to influence the work reported in this paper.

#### Acknowledgements

The authors extend their appreciation to the Deputyship for research & innovation, "Ministry of Education" in Saudi Arabia for funding this research work through the project number IFKSURG-1440-037.

#### References

- Ismail, A., Abdullah, M.J., 2013a. The changes in structural and optical properties of (ZnO:AlN) thin films fabricated at different RF powers of ZnO target. *Ceram. Int.* 39, S441–S445.
- Ismail, A., Abdullah, M.J., 2013b. The structural and optical properties of ZnO thin films prepared at different RF sputtering power. *J. King Saud Univ. – Sci.* 25 (3), 209–215.
- Ismail, A., Abdullah, M.J., 2013c. The effect of substrate temperatures on the structural and optical properties of cosputtered ZnO and AlN thin films. *Adv. Mater. Res.* 626, 25–28.
- Ismail, A., Abdullah, M.J., Qaeed, M.A., 2015. The effect of substrate temperatures on the structural, optical and electrical properties of N-Al codoped ZnO thin films. *J. Luminescence* 164, 69–75.
- Kaschner, A., Haboock, U., Strassburg, M., Strassburg, M., Kaczmarczyk, G., Hoffmann, A., Thomsen, C., 2002. Nitrogen-related local vibrational modes in ZnO:N. *Appl. Phys. Lett.* 80, 1909.
- Alivov, Y.I., Kalinina, E.V., et al., 2003. Fabrication and characterization of n-ZnO/p-AlGaIn heterojunction light-emitting diodes on 6H-SiC substrates. *Appl. Phys. Lett.* 83 (23), 4719–4721.
- Verma, D., Kole, A.K., Kumbhakar, P., 2015. Red shift of the band-edge photoluminescence emission and effects of annealing and capping agent on structural and optical properties of ZnO nanoparticles. *J. Alloys Comp.* 625, 122–130.
- Burstein, E., 1954. Anomalous optical absorption limit in InSb. *Phys. Rev.* 93, 632–633.
- Hezam, M.S., 2007. Synthesis and Characterization of ZnO Thin Films. 2007. Physics. Dhahran, Saudi Arabia, KFUPM. Master of Science.
- Lau, S.P., Yang, H.Y., et al., 2005. Laser action in ZnO nanoneedles selectively grown on silicon and plastic substrates. *Appl. Phys. Lett.* 87 (1).
- M.F. Cerqueira, A.G. Rolo, T. Viseu, J. Ayres de Campos, T. de Lacerda-Arôso, F. Oliveira, M.I. Vasilevskiy, E. Alves, 2010. Raman study of doped-ZnO thin films grown by rf sputtering. *Phys. Status Solidi (c)*, (7) 2290–2293.
- M. Kumar, S.-K. Kim, S.-Y. Choi, 2009. Formation of Al-N co-doped p-ZnO/n-Si (100) heterojunction structure by RF co-sputtering technique. *Appl. Surface Sci.* (256) 1329–1332.
- Ohgaki, T., Ohashi, N., et al., 2003. Growth condition dependence of morphology and electric properties of ZnO films on sapphire substrates prepared by molecular beam epitaxy. *J. Appl. Phys.* 93 (4), 1961.
- Ozgur, U., Alivov, Y.I., et al., 2005. A comprehensive review of ZnO materials and devices. *J. Appl. Phys.* 98 (4), 041301–42103.
- Rusu, G.G., Girtan, M., et al., 2007. Preparation and characterization of ZnO thin films prepared by thermal oxidation of evaporated Zn thin films. *Superlatt. Microstruct.* 42 (1–6), 116–122.
- Ryu, Y.R., Zhu, S., 2000. Optical and structural properties of ZnO films deposited on GaAs by pulsed laser deposition. *J. Appl. Phys.* 88 (1), 201.
- Moss, T.S., 1954. The interpretation of the properties of indium antimonide. *Proc. Phys. Soc. London Ser. B* 67, 775.
- Yamamoto, T., 2002. Codoping for the fabrication of P-type ZnO. *Thin Solid Films* 420, 100.
- Kumar, V., Kumar, V., Som, S., Duvenhage, M.M., Ntwaeaborwa, O.M., Swart, H.C., 2014. Effect of Eu doping on the photoluminescence properties of ZnO nanophosphors for red emission applications. *Appl. Surface Sci.* 308, 419–430.
- Zi-qiang, X., Hong, D., Yan, L., Hang, C., 2006. Al-doping effects on structure, electrical and optical properties of c-axis-orientated ZnO: Al thin films. *Mater. Sci. Semicond. Process.* 9, 132–135.
- Zhao, Y., Li, Z., Lv, Z., Liang, X., Min, J., Wang, L., Shi, Y., 2010. A new phase and optical properties of the N-doped ZnO film. *Mater. Res. Bull.* 45, 1046–1050.